Technical Note

Optimal sample preparation for the analysis of micrometric heterogeneous samples

Victòria Beltran, Nati Salvadó, Salvador Butí, Gianfelice Cinque, Katia Wehbe, and Trinitat Pradell

Anal. Chem., **Just Accepted Manuscript** • DOI: 10.1021/acs.analchem.5b01997 • Publication Date (Web): 29 May 2015

Optimal sample preparation for the analysis of micrometric heterogeneous samples

Victòria Beltran[1,4], Nati Salvadó[1,4*], Salvador Butí[1,4], Gianfelice Cinque[2], Katia Wehbe[2], Trinitat Pradell[3,4]

1. Dpt. d'Enginyeria Química. EPSEVG. Universitat Politècnica de Catalunya, Av. Víctor Balaguer s/n, 08800 Vilanova i la Geltrú, Barcelona
2. Diamond Light Source, Harwell Campus, Chilton-Didcot OX11 0DE Oxon, U.K.
3. Dpt. Física. Universitat Politècnica de Catalunya. Campus del Baix Llobregat, c. Esteve Terradas 8, 08860 Castelldefels, Barcelona and
4. Center for Research in Nano-Engineering, Universitat Politècnica de Catalunya, Barcelona, Spain

* Corresponding author:
E-mail address: nativitat.salvado@upc.edu
Telephone: 0034938967717
Fax: 0034938967700

ABSTRACT

Precise microanalytical techniques are essential in many fields such as Cultural Heritage materials, showing complex layered microstructures containing a wide range of materials of diverse nature and hardness. Non-invasive sample manipulation and preparation is required to avoid, as far as possible, sample contamination which may strongly limit the materials identification.

The method proposed consists in the application of thin gold or carbon protecting layers before embedding the samples in synthetic resin for microtoming. The validity and optimal procedure is checked for those materials most often found on the paintings surface: varnishes (natural resins and wax).

An artwork sample is similarly prepared and analysed by Optical Microscopy (OM), Scanning Electron Microscopy (SEM/EDS), Micro Infrared Spectroscopy (μFTIR/ μSR-FTIR) and X-Ray diffraction (μSR-XRD) with synchrotron light.

INTRODUCTION

Precise microanalytical techniques are essential in many fields and in particular for the study of Cultural Heritage materials. The samples often show a complex layered microstructure containing a wide range of materials of diverse nature and hardness which requires of accurate sample manipulation and preparation. Non-invasive sample preparation is required to avoid the sample contamination which may strongly limit the materials identification. Different strategies are used to assist sample manipulation; among them, one of the most common is to embed fragments in a supporting medium [1]. This procedure helps handling even the tiniest and most fragile samples for polishing or microtoming. Polished cross sections and thin preparations are needed to analyse the layer microstructure by means of Optical Microscopy (OM), Scanning Electron Microscopy (SEM/EDS), Infrared Spectroscopy

FTIR, Raman spectroscopy, X-Ray Fluorescent Spectroscopy (XRF) or X-Ray diffraction (XRD) [2-6].

The requirements of an optimal embedding medium for micrometric heterogeneous samples such as those found in Cultural Heritage materials (paintings, furniture, leather…) have been widely discussed elsewhere [7-9]. A good embedding medium must be transparent (needed for localizing the area of interest), hard enough to be cut and polished, should not shrink during curing, cure at room temperature (some materials are easily damaged by temperature changes) and should not react or penetrate the sample. Other desirable features are low toxicity, low cost and a fast curing.

Among those requirements, the penetration of the embedding medium in the sample surface may interfere with the analysis, and is especially important for organic compounds analysed by FTIR or Raman spectroscopy where it gives a strong signal.

Despite a perfect embedding medium has yet to be discovered the most commonly used is a synthetic resin, primarily epoxy or polyester. Both match the requirements quite well except for the low reactivity and penetration capability [6, 10-15]. Other synthetic resins, such as acrylic, cyanoacrylate or polyethylene based polymer, have neither a lower reactivity nor a lower penetration and display more limitations with the other requisites. [7]

Mathematical subtractions have been tested to remove the embedding medium contribution in the contaminated sample spectra [9]; but to define a precise method has proved to be difficult and may lead to wrong conclusions. Another strategy is to minimize the embedding medium infiltration, which may be attained by protecting the surface by a coating layer. However, this is problematic as the embedding medium acts also as a consolidator and aids cutting, polishing or microtoming fragile samples which otherwise may easily crumble. Despite the difficulties, some smart approaches are giving promising results. Full substitution of the synthetic resin by an IR-transparent salt has been tested, but the block obtained is more brittle and forbid the use of water lubricated diamond saws or polishers [9]. Sample coatings, which do not interfere with sample analysis such as molten or dissolved organic media layers (wax, gels, cyclododecane etc) [7, 10] and metallic coatings [11] have also been considered. The simplest and least invasive method is the application of a gold coating (5 nm), which has already been tested in comparative studies but no in a deep monographic research [7, 16]. Gold sputtered coatings offer many advantages: they are easy and fast to apply, non-toxic and do not react or interfere with the sample; consequently, in this study we examine the possibilities of thick gold sputtered coating layers to protect the samples from embedding medium contamination. The only handicap of this method is that it disturbs the analysis of those samples already containing gold; for such cases, we also test the protective capability of carbon sputtered coatings.

A large number of materials of interest in Cultural Heritage are varnished, in particular paintings, and consequently the most external layer of the samples is often a varnish. For this reason, we selected those compounds constituting the most common natural varnishes to check the best sample preparation method. Although synthetic materials were also employed as a varnish, their use started in the 19th century.

The penetration of the embedding medium into the sample surface is evaluated by means of µFTIR spectroscopy. µFTIR is known to provide broad species identification with minimal sample area [17-19] of particular interest in the identification of organic compounds [20]. Although different setups are available for FTIR spectroscopy, only the transmission geometry gives the desired sensitivity and spectral quality for unambiguous identification of the substances present. Consequently, the embedding medium contamination is estimated by transmission µFTIR spectroscopy from coated microtomed thin sections of natural varnishes embedded in synthetic resin.

Finally, artwork samples have also been prepared and analysed by µSR-FTIR, µSR-XRD and SEM to demonstrate the potentiality of the sample preparation method proposed.

EXPERIMENTAL SECTION

A series of experiments have been designed to test the protective capability of embedding medium infiltration of gold and carbon coating layers for test materials and artwork samples.

Test materials:
Historic natural varnishes are mainly resins, and occasionally waxes or protein materials. The protein material chiefly used was egg white. Most used wax comes from bees, but shellac wax was also used. The resins are secretions of animal or vegetable origin chemically differentiated into large groups such as sesquiterpenoids (shellac), triterpenoids (mastic and dammar), communic acid based diterpenoids (sandarac, amber and copal) and abietane based diterpenoids (*Pinaceae* resin) [15].

Natural and 15 years aged egg white (room temperature and protected from direct sun light) were selected. Beeswax was obtained from a honeycomb. Shellac wax was purchased at Zecchi (Ref. 2750). Among the resins, dammar was bought at CTS (Ref. 01125501) and sandarac at Zecchi (Ref. 2250); amber, shellac (*gommalacca rubino*) and mastic samples were obtained from particular collections. Finally, *Pinaceae* resin was extracted from a *Pinus Sylvestris* L. (Jardí Botànic de Barcelona).

Artwork samples: One to two hundred micrometres in size samples (all layers over canvas support) were extracted from the Sant Francesc d'Assís life series painted by Antoni Viladomat (1678-1755) and kept in the Museu Nacional d'Art de Catalunya MNAC [21].

Embedding medium: Epoxy and polyester resins were tested.
The polyester resin (CCP Composites), is a copolymer of pthalic anhydride and ethylene glycol with styrene and dicyclopentadiene for cross linking (NORSODYNE® O 12335 AL) catalyzed with a Methyl Ethyl Ketone Peroxide (LUPEROX® K1 G). The unsaturated resin has low viscosity and contains other minor compounds like methyl methacrylate. It needs three days to cure.

The epoxy resin (Resineco, ref. TR KIT), is a copolymer of bisphenol A and epichlorohydrin which has other components such as oxirane and 2-P-tolyloxymethyl-oxirane. It is mixed

with a hardener made of 5-amino-1,3,3-trimethylcyclohexanemethylamine and trimethyl-1,6-hexanediamine producing a cross linked polymer. It needs 24 hours to cure.

To embed the samples, a resin bed of either polyester or epoxy was left to polymerize for 30 minutes and four hours respectively before the samples were placed and covered with resin.

Analytical instrumentation

Infrared spectroscopy: A Bruker Vertex 80 V Fourier Transform IR Interferometer coupled to a Hyperion 3000 microscope with a 20X condenser and a MCT detector was used in transmission mode, 4cm^{-1} resolution and 30x30µm measuring area. A micro compression cell Specac GS02520 with KBr windows of 13x2mm has been used for the analysis of the test materials sections; artwork samples were pressed between two thin KBr (Scharlau PO 01680100) pellets.

Thin sections of artwork samples were analysed by synchrotron-based infrared microspectroscopy (µSR-FTIR) at beamline MIRIAM B22 at Diamond Light Source, UK [22]. The Bruker 80 V Fourier Transform IR Interferometer is equipped with Hyperion 3000 microscope, a broad-band high sensitive MCT detector and a 36x condenser. The spectra were obtained in transmission mode using a small beam spot of 15x15 μm^2, 4 cm^{-1} resolution, co-adding 256 scan at scanner velocity 80 kHz (35 sec), in the 4000 to 650 cm^{-1} range. IR maps of the molecular composition were obtained by scanning the sample via a micrometric resolution motorized X-Y stage.

X ray diffraction: Synchrotron based micro-X-ray diffraction measurements (µSR-XRD) were taken from 20 µm thick cross sections of samples extracted from the artworks at beamline XALOC of the ALBA Synchrotron, Cerdanyola del Vallès (Barcelona) with a focused beam of 50x6µm (FWHM), 1s acquisition time and 12.6 keV energy in a virtually noise free Pilatus 6M (Dectris) detector with a large (424x435 mm^2, 6 Mpixels) active area [23].

Scanning Electron Microscope: measurements were made by means of a GEMINI SEM equipment with a Shottky-FE column at 4pA-20 nA, 0.1 to 30 kV and 1nm resolution for 20KV. Elemental analysis was made with an EDS with an INCAR Penta FETX3 detector and a 30 mm^2 ATW2 window.

For additional technical details related to protective gold and carbon coatings and microtomed samples see supporting information (table S1)

RESULTS AND DISCUSSION

Embedding medium

Natural varnishes were embedded in epoxy and polyester resin to test the best embedding medium. Although between 8µm and 1µm thick sections could be obtained from both, epoxy is more transparent and the slices are more easily cut and consistent. Polyester is more fragile and is often fragmented during microtoming; sections obtained are sticky, easily broken and it is convenient to analyze them immediately after cutting. Some thin sections are showed in supporting information (Fig. S2)

Thickness optimization

8, 5, 2 and 1μm thick sections of all compounds were cut to determine the optimal sample thickness for μFTIR transmission analysis. As an example, μFTIR spectra corresponding to shellac are shown in supporting information Fig. S3. The optimal thickness is assessed from the absorption data and corresponds to those sections of thickness varying between 5μm and 2μm; thicker sections produce saturated spectra and although 1μm thick sections give good IR spectra, they are extremely fragile and are difficult to obtain and keep in good agreement with other studies [7, 11, 24, 25].

We have to mention that the molar absorptivity is compound dependent, for this reason it was also measured for those compounds with suitable properties for making pellets and was taken into account in the analysis of the data. Mastic shows the highest molar absorption, amber and dammar the lowest and sandarac shows different values depending on the wavenumber. (See supporting information Fig. S3)

Embedding medium infiltration

The corresponding IR spectra for polyester and epoxy can be seen in supporting information (Fig. S4). Epoxy appears very suitable for embedding natural varnishes because the band with the highest absorbance appears at 1510 cm^{-1} for which most materials commonly used as natural varnishes are band free. Epoxy has also a medium intensity double peak at 1608 and 1580 cm^{-1} which can be used as a specific marker for detecting its presence (all bands are associated to the stretching of aromatic groups) [26-29]. Conversely, the IR spectrum of polyester has the highest absorbance at 1731 cm^{-1} (associated to the stretching of C=O bond [21, 30]), overlapping with many important bands of the varnishes. A double band at 1600 and 1580 cm^{-1} (associated to the stretching of aromatic groups [21, 22]) which could be used as a specific marker for detecting polyester contamination has a low intensity that makes it unsuitable for low contamination cases. This is probably one of the weakest points of polyester resin.

The results obtained show that, generally speaking, polyester penetrates deeper in the samples than epoxy for equivalent coatings, as is shown in (Fig. 1). In particular, Fig. 1a shows the case of shellac wax protected with the thinnest carbon coating. Measurements taken immediately below the sample surface (spectra I and III) are compared with the spectrum of shellac wax (spectrum II). As it can be seen in fig. 1a, the intensity of the epoxy markers is really low (the slight increase observed at the 1737 cm^{-1} band is related to the decrease of shellac wax concentration because of epoxy penetration). Contrariwise, polyester markers show a higher intensity, the shoulder at 1285 $cm^{-1}$and the contribution at 1731 cm^{-1} which overlaps with some bands corresponding to the shellac wax: curve fitting has been applied to resolve this band from the polyester band intensity (Fig. 1a, VII). The distortion produced by the presence of other bands related to polyester is also observed.

Fig. 1b shows the same than Fig. 1a but corresponding to sandarac (spectra IV, V and VI). The spectrum of sandarac embedded in epoxy resin shows a medium intensity band at 1510 cm^{-1} which is directly related to the epoxy concentration. The intense shoulder at 1730 cm^{-1} overlapping the 1694 cm^{-1} sandarac band is related to the presence of polyester; curve fitting shown in (Fig. 1b, VIII) demonstrates the importance of the polyester band. Therefore,

we can conclude that the polyester concentration is higher than the epoxy for equivalent sandarac sample preparations.

The larger penetration of polyester can be explained because, polyester needs longer time to be cured than epoxy (polyester cures in three days and epoxy in 24 hours) and polyester monomers are smaller than epoxy's.

Epoxy resin is less invasive; consequently, the other comparative studies (infiltration of the resin depending on the test material embedded and the protective coating) were performed with epoxy resin only. From them, we can state that the embedding medium penetration is a real problem that may distort the spectra of the external layers (in some cases the embedding resin may penetrate as deep as 20μm) (see supporting information, Fig. S4-S14).

Although all the coatings considered reduce the embedding medium contamination, gold is the best. Gold protects extremely well egg white, mastic, shellac and shellac wax. With other materials such as amber, sandarac and fresh *Pinus* resin, the contamination affects very little the IR spectra. Although even gold does not reduce impressively the epoxy penetration in dammar, it protects the surface reasonably well. Finally, despite carbon is less effective, occasionally, as happens for shellac and beeswax, it is enough to decrease substantially the embedding medium contamination (see supporting information, Fig. S15). Differences between test materials results can be explained because of its different molar absorptivity.

Artwork sample analysis

Protective coatings were also tested for artwork microsamples. A small fragment (125x200x400 microns) of a blue painting was gold-coated (40 to 60 nm) and embedded in epoxy resin; 2μm thick cross sections were cut with the microtome. The sample selected is particularly complex formed by various compounds of very different hardness. The thin cross section (Fig 2a) shows a brown preparation layer (>150 μm) containing calcium carbonate (calcite $CaCO_3$), clay minerals (illite and kaolinite), quartz, iron oxides (hematite) and calcium oxalates (weddellite), followed by a layer of lead white (mainly cerussite $PbCO_3$ with a small amount of hydrocerussite $2PbCO_3{\cdot}Pb(OH)_2$) mixed with carbon black particles (15-20 μm); over it, a lead white paint with smalt blue particles (~30μm) and a diterpenic varnish (<4μm).

The microtome cut exposes a polished sample surface, free of cutting and polishing contamination (diamond, alumina, silicon carbide, etc.). This surface is adequate for SEM observation and analysis (Fig. 2b) [31]. The backscattering image (Fig. 2b) shows each layer and the thin gold protective coating on top of the varnish. The flat surface obtained may also be suitable for other analysis such as μATR-FTIR and Raman spectroscopy. EDS analysis have been used to characterize the blue particles (mainly Si, K, Fe, Co and As as minor components).

Thin cross sections were analysed by μSR-FTIR to determine the embedding medium penetration. The epoxy resin presence has been measured by integrating the double peak at 1608 and 1580 cm^{-1}. (Fig 2c) shows the presence of resin at a depth of 5μm, affecting only the most external varnish layer.

The thin cross section has also been analysed by conventional µFTIR with a Globar light source on 30 μm^2 areas obtaining good quality spectra which permits to determine the layers composition (Fig. 2d). The paint layers show bands characteristic of drying oil, $PbCO_3/2PbCO_3{\cdot}Pb(OH)_2$ and $CaCO_3$. The middle paint layer shows a 1508 cm^{-1} asymmetric stretching (COO^-) band related to lead palmitate produced by the reaction between lead white and drying oil, as shown in spectrum II. Finally the preparation layer shows the bands characteristic of silicates and calcium carbonate.

The thin cross sections are also suitable for µSR-XRD. For this, a 20 µm thick cut of the same fragment was analysed using a 50x6µm spot and taking a measurement every 3µm across the different layers. The crystalline compounds present in the layers are determined as shown in Fig 2e. Neither carbon nor smalt are identified, because the carbon main peaks overlap with those of quartz and smalt is not crystalline. The presence of carboxylates of various natures is also determined in the preparation and both painting layers (Fig. 2e). The peaks corresponding to the carboxylates are broad and may be clearly distinguished because of the large size of those molecules (low diffracting angles). A continuous decrease in the d-spacing values, from the preparation layer (50.573 Å, 25.181 Å, 17.090 Å, 12.110 Å), the first (49.514 Å, 24.472 Å, 16.248 Å, 12.123 Å) and the second painting layers (48.898 Å, 24.238 Å, 16.106 Å, 12.110 Å) is observed. Moreover, some new d-spacings are seen at 14.734 Å, 9.649 Å, 7.2520 Å, 6.6393 Å, 4.0726 Å or 3.9246 Å, in the most external painting layer. The largest d-spacings can be related to calcium and lead stearates (about 50 Å and 25 Å), smaller values to palmitates (about 45 Å and 23 Å) [32]. Previous results demonstrate also that the lead and calcium carboxylates formed due to the reaction of lead white or calcium carbonate with drying oil show intermediate d-spacings between those of stearate and palmitate. The potassium stearates have also smaller d-spacings comparable to those of calcium and lead palmitates. The small d-spacings, as well as, the formation of a second set of d-spacings in the most external painting layer could be related to the formation of potassium and lead mixed carboxylates; potassium originating from the smalt particles present in the second painting layer. More work should be devoted for a full identification of carboxylates and their relationship with the paintings conservation.

CONCLUSIONS

The sample preparation methodology proposed consisting in, first the application of a gold coating, then epoxy resin embedding and finally microtoming (between 20 to 2µm) has proved to be very successful for the analysis of painting heterogeneous fragile microsamples. Gold and carbon were tested as coating metals, and although both work, gold is more protective. Epoxy and polyester resins were tested as embedding medium, among them epoxy has proved to give the best protection and the necessary consistency for cutting. Moreover, epoxy is easily detected in varnished samples of maximum interest in the study of cultural heritage materials. These results cast an interesting approach and its application to other heterogeneous fragile microsamples could be assessed in future research.

Finally, it is important to highlight that the same preparation may be used for μFTIR, μXRD, μXRF, Raman, SEM-EDS and MO. The potentiality of the methodology is demonstrated in the analysis of an artwork sample with micro layered structure including a wide range of materials, original organic and inorganic pigments and binders, and reaction, aging and weathering products.

SUPPORTING INFORMATION AVAILABLE

This material is available free of charge via the Internet at http://pubs.acs.org.

ACKOWLEDGEMENTS

The work received financial support from MICINN (Spain), MAT2013-41127-R and Generalitat de Catalunya, 2014SGR-581 grants. We would like to thank Diamond Light Source for allowing access to beamline MIRIAM B22 (SM10400) and also the funding from FP7/2007-2013 under grant agreement nº 226716. The μSR-XRD experiments were performed at BL13 XALOC beamline at ALBA Synchrotron with the collaboration of ALBA staff in particular Jordi Juanhuix.

The authors would also like to thank Trifon Trifonov Todorov, from CRNE (UPC) for his help with sample coating, the Museu Nacional d'Art de Catalunya, MNAC, for access to the art works, David Bertran curator of "Jardí Botànic de Barcelona" for supplying the *Pinaceae* resin and the Master Violin Maker, José María Lozano, for supplying the amber and shellac resins.

REFERENCES

(1) Plesters, J. *Stud. Conserv.* **1956**, 2, 3, 110-157.
(2) Doménech-Carbó, M. T. *Anal. Chim.Acta.* 2008, 621, 109-139.
(3) Sandu, I.; Schäfer, S.; Magrini, D.; Bracci, S.; Roque, C. *Microsc. Microanal.* **2012,** *18*, *4*, 860-75.
(4) Bertrand, L.; Robinet, L.; Thoury, M.; Janssens, K.; Cohen, S. X.; Schöder, S. *Appl. Phys.* A 2012, 106, 2, 377-396.
(5) Salvadó, N.; Butí, S.; Aranda, M. A. G.; Pradell, T. *Anal. Methods* **2014**, *6*, 3610-3621.
(6) Salvadó, N.; Butí, S.; Pantos, E.; Bahrami, F.; Labrador, A.; Pradell, T. *Appl. Phys*. A **2007**, *90*, 67-73.
(7) Derrick, M. R.; Souza, L.; Kieslich, T.; Florsheim, H.; Stulik, D. *J. Am. Inst. Conserv.* **1994**, *33*, *3*, 227-245.
(8) Chang, W. T.; Chen, T. H.; Yu, C. C.; Kau, J. Y. *Forensic Sci. J*. **2002**, *1*, 55-60.
(9) Wachowiak, M. J. *J. Am. Inst. Conserv.* **2004**, *43*, *3*, 205-226.
(10) Schmidt-Patterson, C.; Carson, D.; Phenix, A.; Khanjian, H.; Trentelman, K.; Mass, J.; Hirschmugl, C. *e-Preserv. Sci*. **2013**, *10*, 1-9.
(11) Prati, S.; Sciutto, G.; Catelli, E.; Ashashina, A.; Mazzeo, R. *Anal. Bioanal. Chem.* **2013**, *405*, 895-905.
(12) Pilc, J.; White, R.; *National Gallery Technical Bulletin*, **1995**, *16*, 73-84.
(13) Fonjaudran, C. M.; Nevin, A.; Piqué, F.; Cather, S. *Anal. Bioanal. Chem*. **2008**, *392*, 77-86.
(14) Pouyet, E.; Lluveras-Tenorio A.; Nevin A.; Saviello D.; Sette, F.; Cotte M. *Anal. Chim. Acta.* **2014**, *822*, 51-59.
(15) Mills, J.; White, R. *Organic Chemistry of Museum Objects*, 3rd ed.; Butterworth-Heinemann: Ofxord, 1999.
(16) Kopecká, I.; Svobodová, E. *Heritage Science*. **2014**, *2:22*, 1-8

(17) Derrick, M. R.; Landry, J. M.; Stulik, D. C. *Scientific tools for conservation: Infrared Spectroscopy in Conservation Science;* Getty Conservation Institute: Los Angeles, 1991.
(18) Salvadó, N.; Butí, S.; Tobin, M. J.; Pantos, E.; Prag, A. J. N. W; Pradell, T. *Anal. Chem*. **2005**, *77*, 3444-3451.
(19) Werd, J.; Heeren, R. M. A.; Boon, J. J. *Stud. Conserv*. **2004**, *49*, 193-210.
(20) Beltran, V.; Salvadó, N.; Butí, S.; Cinque. *Microchem. J.* **2015**, *118*, 115-123.
(21) http://www.museunacional.cat/
(22) Cinque, G.; Frogley M.; Wehbe, K.; Filik, J.; Pijanka, J.; *Diamond Synchrotron Radiation News* **2011**, *24*, 24–33.
(23) Juanhuix, J.; Gil-Ortiz, F.; Cuni, G.; Colldelram, C.; Nicolas, J.; Lidon, J.; Boter, E.; Ruget, C.; Ferrer, S.; Benach, J. *J. Synchrotron Rad.* **2014**, *21*, 679-689.
(24) Echard, J. P.; Cotte, M.; Dooryhee, E.; Bertrand, L. *Appl. Phys. A*. **2008**, *92*, *1*, 77-81.
(25) Lluveras-Tenorio, A.; Andreotti, A.; Bonaduce, I.; Boularand, S.; Cotte, M.; Roqué, J.; Colombini, M. P.; Vendrell-Saz, M. *Chem. Cent. J*. **2012**, *6*, *45*, 1-18.
(26) Bolasodun, B.; Rufai, O.; Durowaiye, S. *Int. J. Eng. Sci.* **2014**, *3*, *1*, 11-23.
(27) Farhadyar, N.; Rahimi, A.; Langroudi, A. E. *Iran. Polym. J.* **2005**, *14*, *2*, 155-162.
(28) Nikolic, G.; Zlatkovic, S.; Cakic, M.; Cakic, S.; Lacnjevac, C.; Rajic, Z. Sensors **2010**, *10*, 684-696.
(29) Bellamy,L. J.; *The infrared spectra of complex molecules*, 3rd ed., Halsted Press: New York, 1975.
(30) Knuutinen, U.; Kyllonen, P. *e-Preserv. Sci*. **2006**, *3*, 11-19.
(31) Echlin, P. Handbook of Sample Preparation for Scanning Electron Microscopy and X-Ray Microanalysis, 1 ed.; Springer: New York, 2009.
(32) Salvadó, N.; Butí, S.; Nicholson, J.; Emerich, H.; Labrador, A.; Pradell, T. *Talanta* **2009**, 79, 419-428.

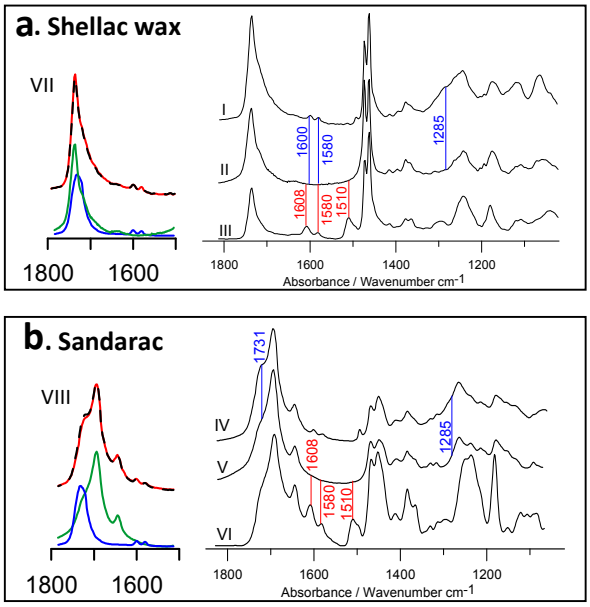

Fig. 1: µFTIR spectra comparison between infiltrations depending on the embedding medium for shellac wax and sandarac. Figure compares reference materials (II and V) with samples embedded in polyester (I and IV) and samples embedded in epoxy (III and VI). For an easy interpretation band at 1700 has been deconvoluted (VII and VIII, blue line: polyester, green line: sample, red line: calculated spectrum, black dotted line: experimental spectrum).

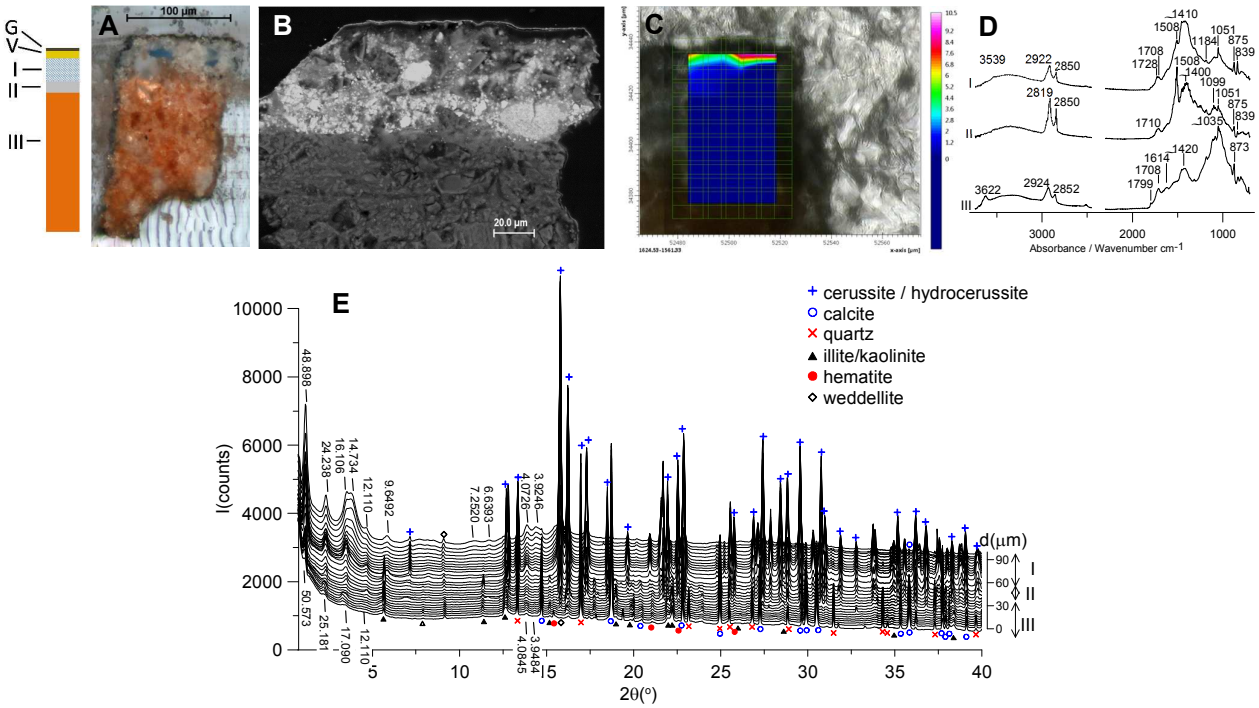

Fig. 2: Artwork sample analysis. a) Thin section with stratigraphy scheme (G= gold coating, V= varnish, I= first chromatic layer II= second chromatic layer III= preparation layer) b) SEM image from the bulk c) µSR-FTIR analysis of epoxy infiltration, the map represents the integration of epoxy doublet at 1608 and 1580 d) µFTIR analysis from layer I, II and III e) µSR-XRD diffraction from layer I, II and III.

for TOC only

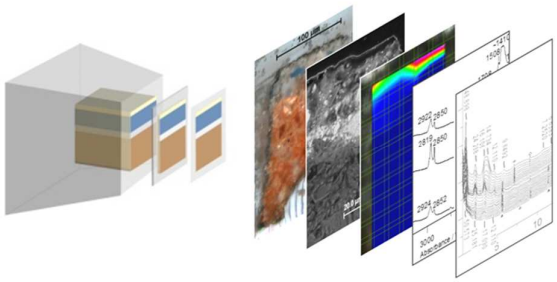

Optimal sample preparation for the analysis of micrometric heterogeneous samples

Victòria Beltran[1], Nati Salvadó[1*], Salvador Butí[1], Gianfelice Cinque[2], Katia Wehbe[2], Trinitat Pradell[3,4]

1. Dpt. d'Enginyeria Química. EPSEVG. Universitat Politècnica de Catalunya, Av. Víctor Balaguer s/n, 08800 Vilanova i la Geltrú, Barcelona
2. Diamond Light Source, Harwell Campus, Chilton-Didcot OX11 0DE Oxon, U.K.
3. Dpt. Física. Universitat Politècnica de Catalunya. Campus del Baix Llobregat, c. Esteve Terradas 8, 08860 Castelldefels, Barcelona
4. Center for Research in Nano-Engineering, Universitat Politècnica de Catalunya, Barcelona, Spain

* Corresponding author:
E-mail address: nativitat.salvado@upc.edu
Telephone: 0034938967717
Fax: 0034938967700

Table of contents:

S-1 Experimental details (additional information)

Turbo evaporator

Protective gold and carbon coatings were applied with a turbo evaporator Emitech K950X using a vacuum of $3x10^{-3}$ mbar.

Carbon coatings were obtained from graphite rods (Ted Pella, product 61-15, grade 1, 1/8" x12"). Two kinds of coatings were produced: thin and thick coatings obtained after 13 and 28 discharges respectively (900ms each discharge, coatings thickness are approximately from 30 to 40 nm and from 60 to 80 nm). Gold coatings were obtained from a 4cm gold strand of 0.08'' diameter purchased at Ted Pella (Ref. 21-10) after two discharges (from 20 to 30 nm coatings thickness). Three sets of preparations, one covered with a thin carbon layer, another covered with a thick carbon layer and a third one covered with gold were obtained. Artwork samples were also gold-coated with four repetitions to ensure a better protection (40 to 60 nm). Pressure changes happening in the turbo evaporator are likely to eject small samples. Thus, an adhesive (Sylgard 184, ref. 761036-1EA from Sigma Aldrich) placed in a small box was used to hold the samples in the evaporator chamber. Afterwards, the samples were mechanically removed from the adhesive using tweezers. The uncoated part of the sample was kept and used to check the efficiency of the coating.

Microtome

The microtome is a Motorized Rotary Microtome RMC MT-990, with a tungsten carbide blade. Despite the difficulties found in some cases sections from all the materials embedded were obtained. The most uniform sections were obtained using a cutting angle of 12^{o}.

Optical Microscopy (OM)

Microsamples were manipulated under a Stereomicroscope, SMZ800 Nikon. Sections and thin slides were observed with an Optical microscope Eclipse LV100 Nikon.

Data Processing

All the collected infrared spectra were processed with Opus 7.2 (Bruker Optics, Inc). Spectra were taken for each test material, embedding medium and coating layer from an area immediately under the sample surface, at 10 μm and at 20 μm depth. At least 3 spectra were obtained at each depth. The region between 1700 and 900 cm^{-1} was selected for data treatment: baseline correction (scattering correction with 64 baseline points) and normalization were first applied. Then, all the spectra corresponding to the same depth were averaged and the standard deviation calculated. In addition, the absorbance of the materials was measured from pellets obtained diluting the compounds with KBr.

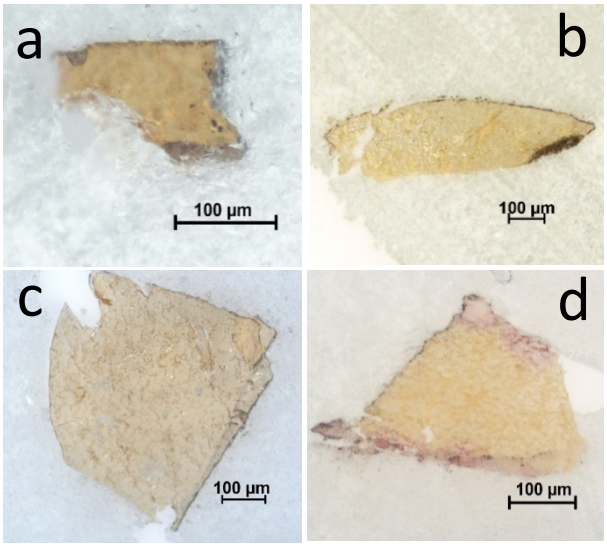

Fig. S2: MO images with polarized light thin sections of shellac coated with a) a thin carbon coating b) a thick carbon coating c) a gold coating and embedded in epoxy resin and d) a thin carbon coating and embedded in polyester resin

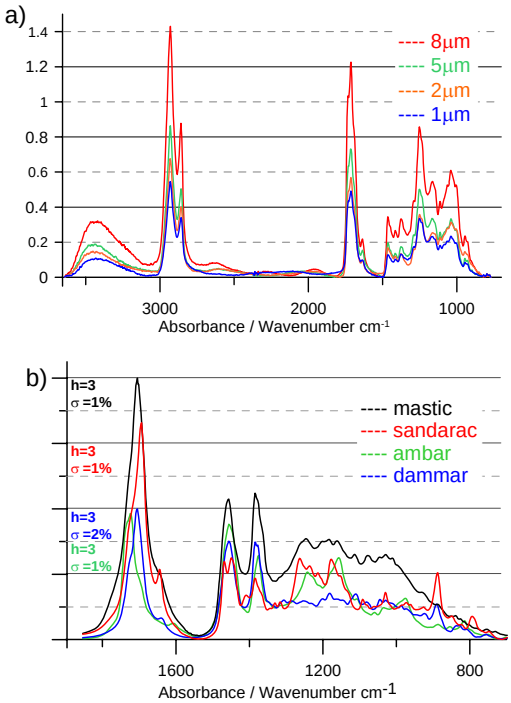

Fig. S3: μFTIR absorbance of a) shellac thin sections of various section thickness and b) various materials (h= number of averaged hits, σ= standard deviation)

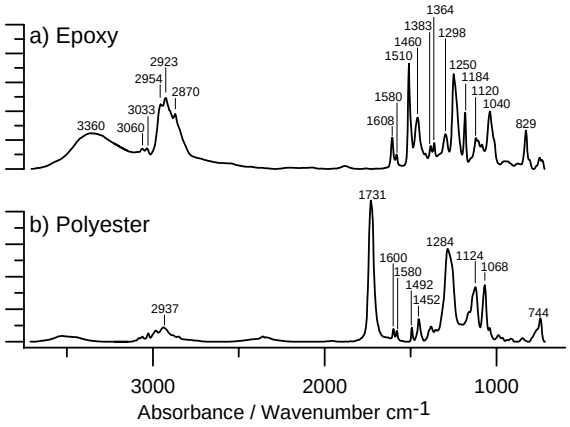

Fig. S4: µFTIR spectra corresponding to the embedding medium tested: a) epoxy and b) polyester resin

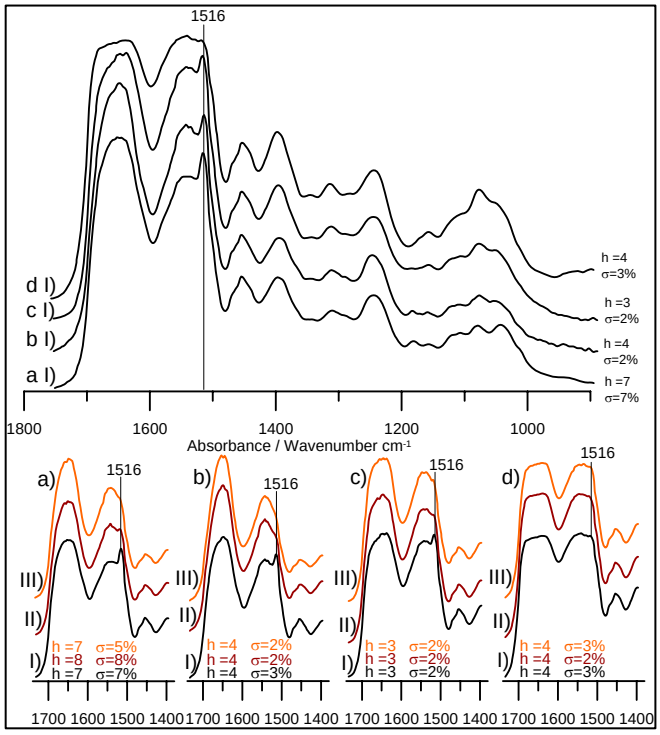

Figure S5: µFTIR spectra of shellac wax a) non-coated sample b) thin coating of carbon c) thick coating of carbon d) coating of gold. I) immediately under the interface with epoxy, II) 10µm under the interface, III) 20µm under the interface

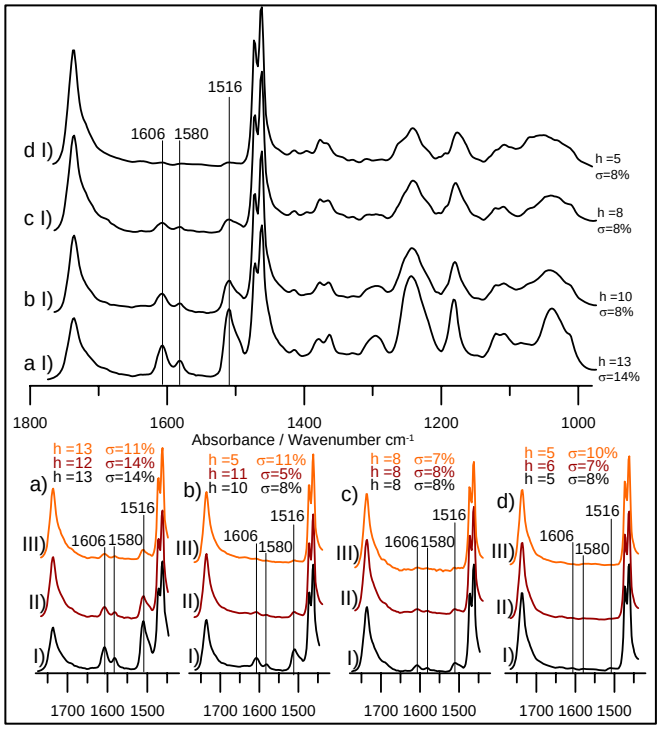

Figure S6: µFTIR spectra of egg white a) non-coated sample b) thin coating of carbon c) thick coating of carbon d) coating of gold. I) immediately under the interface with epoxy, II) 10µm under the interface, III) 20µm under the interface

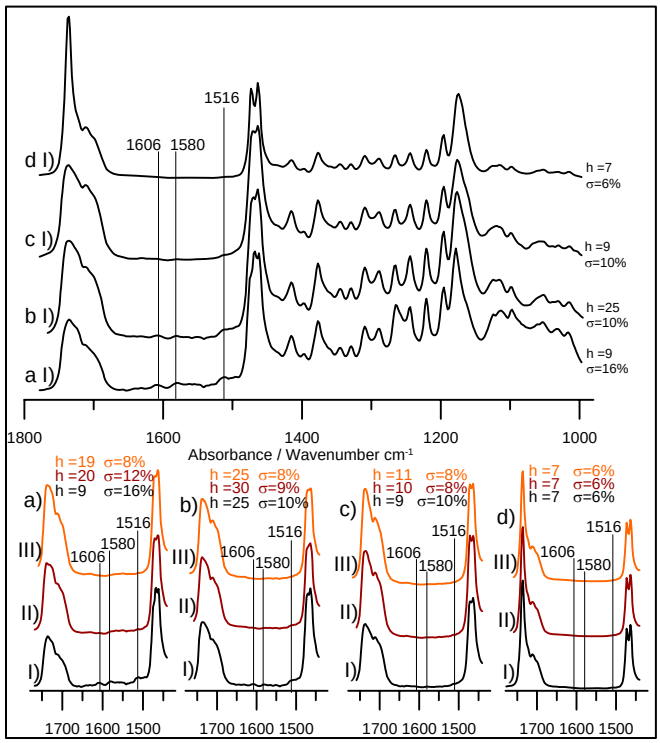

Figure S7: µFTIR spectra of beeswax a) non-coated sample b) thin coating of carbon c) thick coating of carbon d) coating of gold. I) immediately under the interface with epoxy, II) 10µm under the interface, III) 20µm under the interface

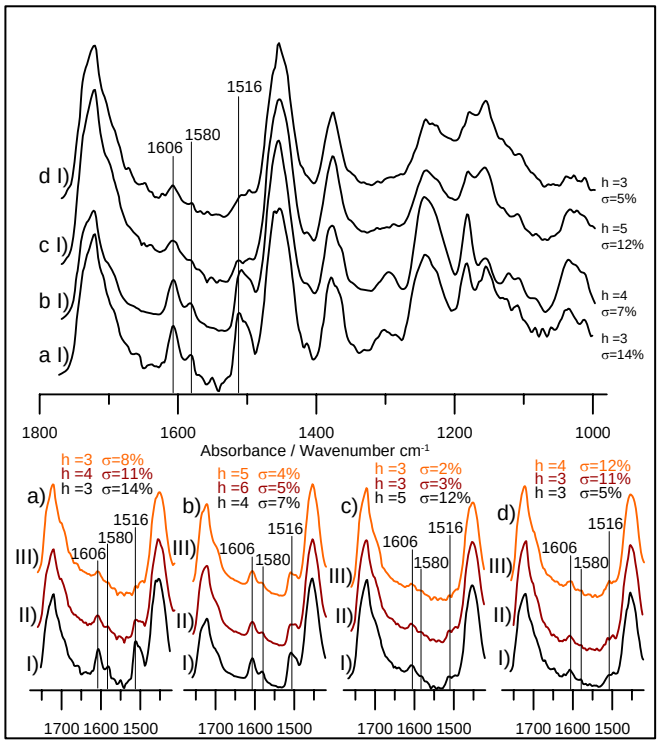

Figure S8: µFTIR spectra of amber a) non-coated sample b) thin coating of carbon c) thick coating of carbon d) coating of gold. I) immediately under the interface with epoxy, II) 10µm under the interface, III) 20µm under the interface

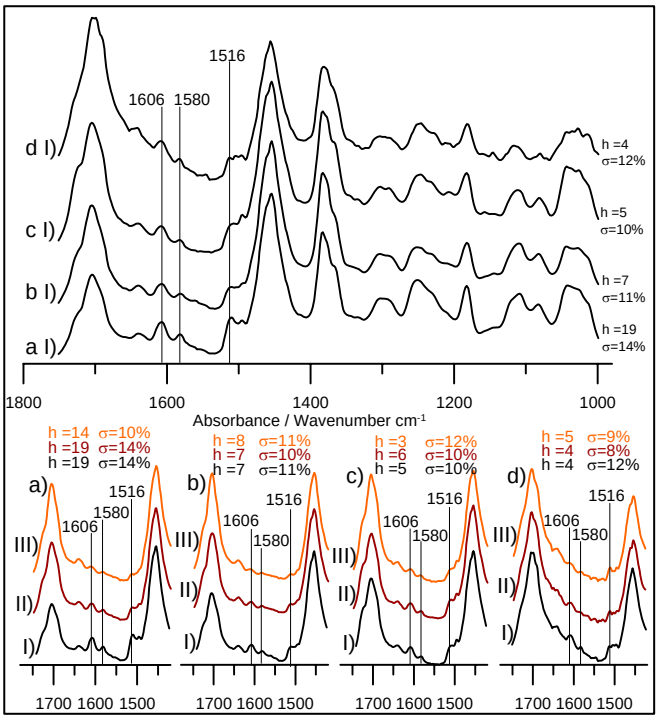

Figure S9: µFTIR spectra of dammar a) non-coated sample b) thin coating of carbon c) thick coating of carbon d) coating of gold. I) immediately under the interface with epoxy, II) 10µm under the interface, III) 20µm under the interface

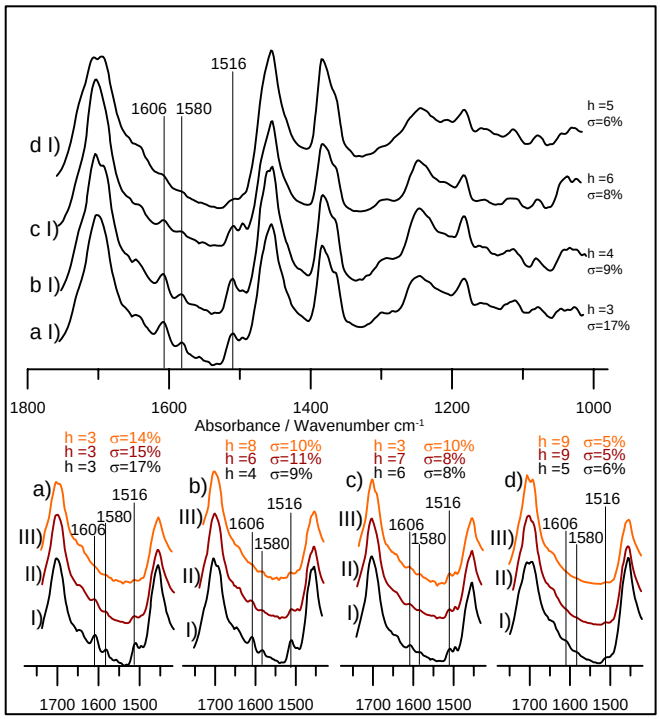

Figure S10: µFTIR spectra of mastic a) non-coated sample b) thin coating of carbon c) thick coating of carbon d) coating of gold. I) immediately under the interface with epoxy, II) 10µm under the interface, III) 20µm under the interface

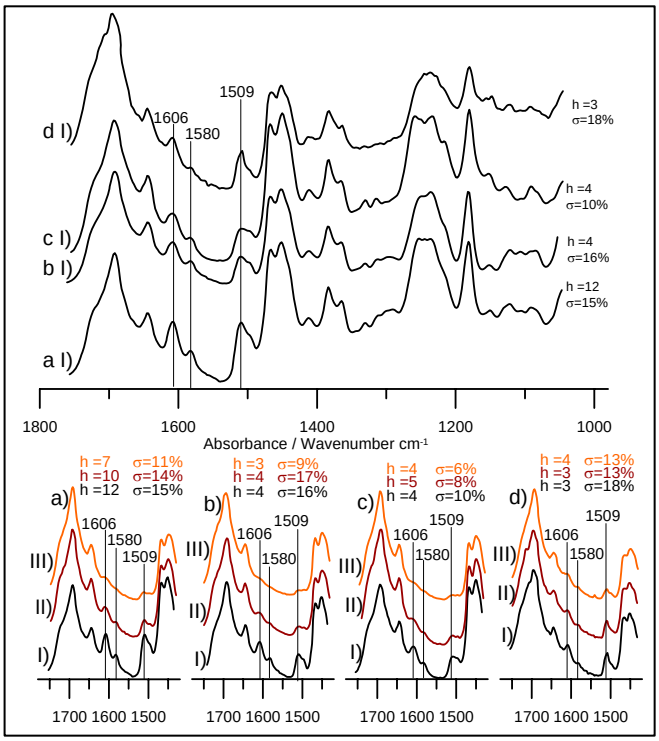

Figure S11: µFTIR spectra of sandaraca a) non-coated sample b) thin coating of carbon c) thick coating of carbon d) coating of gold. I) immediately under the interface with epoxy, II) 10µm under the interface, III) 20µm under the interface

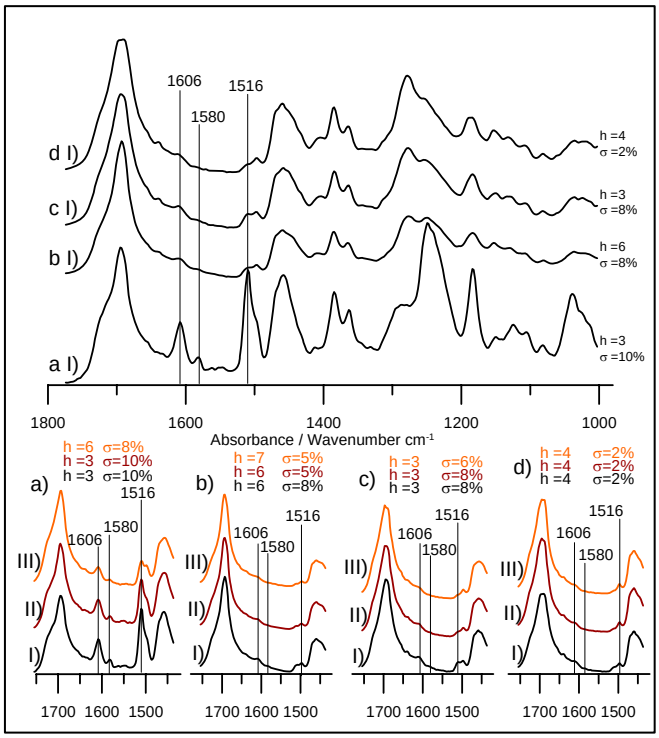

Figure S12: µFTIR spectra of fresh Pinus resin a) non-coated sample b) thin coating of carbon c) thick coating of carbon d) coating of gold. I) immediately under the interface with epoxy, II) 10µm under the interface, III) 20µm under the interface

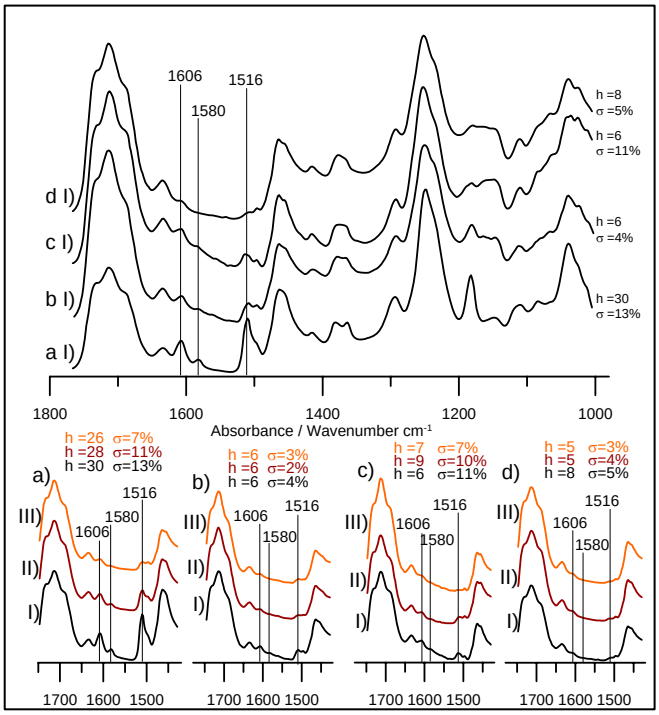

Figure S13: µFTIR spectra of shellac a) non-coated sample b) thin coating of carbon c) thick coating of carbon d) coating of gold. I) immediately under the interface with epoxy, II) 10µm under the interface, III) 20µm under the interface

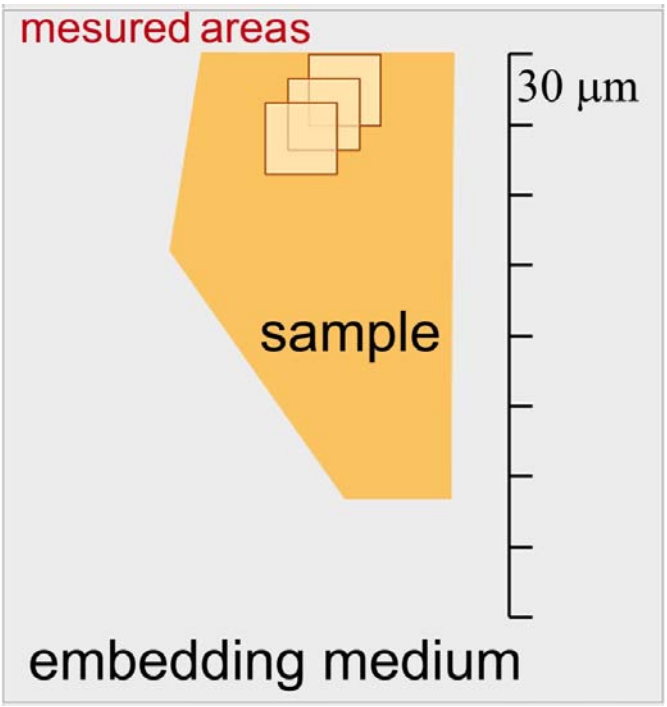

Figure S14: scheme of analyzed areas in a sample section (4µm in thickness). First one was immediately under the sample surface, second one was taken 10 µm under the sample surface and the last one at 20µm.

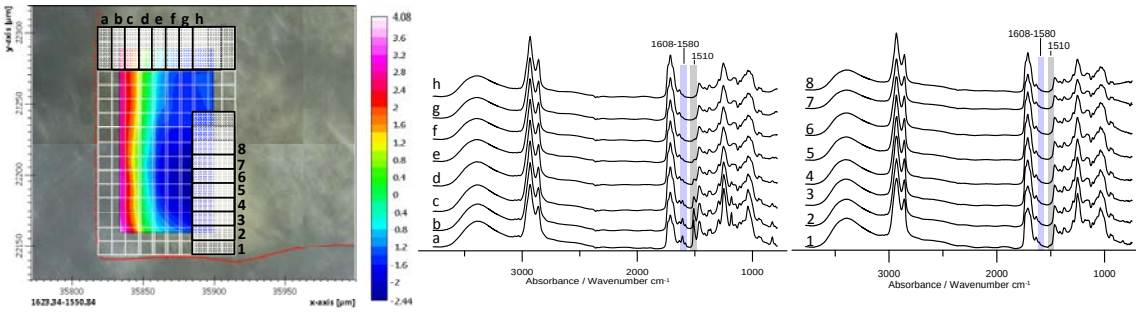

Fig. S15: Left picture: shellac section, dotted red line is in the non coated side and continuous red line is in the coated side (thin carbon coating). The map belongs to the integration of the epoxy double peak at 1608 and 1580 cm^{-1}). Two series of spectra taken at increasing distances from the interface between shellac and epoxy can be seen: series of spectra in a non-coated side (central figure, a-h) and in a coated side (right figure 1-8), specific markers from epoxy have been highlighted.